Proceedings of the 16th International Conference on Soil Mechanics and Geotechnical Engineering

doi:10.3233/978-1-61499-656-9-929

Large compression of soil due to decay of structure during drained repeated shearing

Compression des sols à grande échelle résultant de l'effondrement du squelette structurel du sol

M. Nakano, A. Asaoka, K.Nakai & M. Tashiro
Department of Civil Engineering, Nagoya University, Japan

ABSTRACT

Huge volume compression of loose sand can be easily observed not under monotonic loading but under repeated shear stress application with small amplitudes, which is called compaction of sand. Although it takes long time the similar phenomenon is commonly observed even in highly structured natural clay, which has been called, for long years, secondary consolidation/delayed compression of natural clay. This study describes that these large-scaled volume compression observed both in clay and sand is due to the decay/collapse of soil skeleton structure that occurs with on going plastic shear deformation. Distinguishing the mechanical difference between sand and clay, the super/subloading elasto-plastic constitutive model still explains the mechanism of the volume compression of soils consistently.

RÉSUMÉ

Une compression de volume considérable peut être facilement observée non sous chargement monotonique mais sous l'effet de l'application de contraintes de cisaillement de faible amplitude répétées, connue sous le nom de compactage du sable. Bien qu'il faille du temps, le même phénomène peut être normalement observé avec l'argile naturel à forte structure, ce que pendant longtemps on a appelé la consolidation secondaire/compression différée de l'argile naturelle. Cette étude montre que la compression de volume à grande échelle observée à la fois pour l'argile et pour le sable résulte de l'altération/effondrement de la structure en squelette du sol qui se produit avec la déformation par cisaillement plastique qui s'effectue. Tout en faisant une différence mécanique entre le sable et l'argile, le modèle constitutif élasto-plastique de super/souschargement permet d'expliquer de mécanisme constant de compression de volume des sols.

1 INTRODUCTION

The soil in a naturally deposited foundation, whether clayey or sandy in character, is generally in a developed state of "structure." Also, it is often in an overconsolidated state, as well as being advanced in anisotropy. With regard to these three properties of structure, overconsolidation and anisotropy, two observations can be said to be of great importance for explanatory purposes. Taking clay as our example: (1) Overconsolidation as a result of unloading, and anisotropy as a result of anisotropic consolidation can both be produced, even in normally isotropically consolidated remolded clay, by mechanical manipulations; but it is difficult to create structure by means of such mechanical methods alone. For this reason, the primary difference usually drawn between remolded and naturally deposited clay lies in the presence or absence of structure. (2) Like void ratio etc., structure, overconsolidation and anisotropy are expressions of the mechanical state of a soil. This means in particular that decay of structure (so-called "disturbance"), transition from an overconsolidated to a normally consolidated state (loss of overconsolidation), and change in anisotropy, all occur as the result of loading with plastic deformation.

In Japan as elsewhere, it has long been known that if a sample of naturally sedimented clay is brought into a heavily overconsolidated condition through a release of in-situ stress, the reconsolidation of the soil from the overconsolidated to the normally consolidated state will inevitably lead to a certain amount of disturbance. But, as we have noted, soil disturbance (decay of structure) cannot very well come about except through plastic deformation. Accordingly, the associated transition from the overconsolidated state to the normally consolidated state which co-occurs with disturbance also seems most readily understandable as an accompanying effect of plastic deformation. This insight first found formal expression in Hashiguchi's concept of the subloading yield surface (Hashiguchi, 1989). As will be explained in this paper, the above observations (1) and (2) apply equally well in the case of sand.

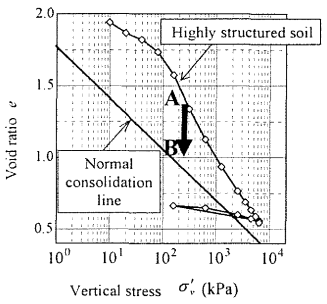

Figure 1. One-dimensional compression behavior of structured clay.

In addition to what has been argued concerning points (1) and (2), (3) we first show how a decay of structure brings the volumetric compression of the soil. We then show how it is possible for this volumetric compression to be induced through repeated shearing under drained conditions, with no requirement for an increase in the mean effective stress. Finally, it is stressed that this observation (3) is as valid for sand as it is for clay, and is of great significance both for the compaction behavior of sand and for the consolidation behavior of clay. It should be noted here also that Asaoka et al. (2000), on the basis of Fig. 1 for the case of a clay soil, accounted for "structure" as the "bulk condition" of the soil and introduced the explicatory concept of a superloading yield surface. In purely verbal terms, it is easy to appreciate how the progressive decay of bulk results in volumetric compression. Yet this figure on its own is insufficient to explain the course of the path that leads from A to B.

2 SUPER/SUBLOADING YIELD SURFACE CAM-CLAY MODEL

The super/subloading yield surface model (Asaoka et al., 2002) was developed to account for structure, overconsolidation and anisotropy. As it also provides the main basis for the observations to be made in the present paper, let us begin by giving an outline of it, together with a summary of its main characteristics.

2.1 *The plastic potential, evolution laws and constitutive equation*

The behavior of a remolded soil, displaying neither structure nor overconsolidation, is described by the modified Cam-clay model. Anisotropy is expressed and incorporated into the modified Cam-clay model under a concept of rotational hardening involving the stress parameter η^* (Sekiguchi & Ota, 1977) and its evolution (Hashiguchi & Chen, 1998). Above the plastic potential (or "normal-yield" surface) of the Cam-clay model, structure is then expressed by superposing an analogous superloading surface (similarity ratio R^*, $0 < R^* \leq 1$, definition Fig. 2), while overconsolidation is expressed by the further addition of an analogous subloading surface (similarity ratio R, $0 < R \leq 1$, Fig. 2) on the underside of the superloading surface. Eq. (1) thus expresses the subloading surface, on which the current stress state always lies, while Eq. (2) expresses the normal-yield surface.

$$f(p',\eta^*) + \mathrm{MD}\ln R^* - \mathrm{MD}\ln R + \int_0 J\mathrm{tr}\boldsymbol{D}^p d\tau = 0 \tag{1}$$

$$f(\tilde{p}',\eta^*) = \mathrm{MD}\ln\frac{\tilde{p}'}{\tilde{p}'_0} + \mathrm{MD}\ln\frac{\mathrm{M}^2+\eta^{*2}}{\mathrm{M}^2} (= \varepsilon_v{}^p) = -\int_0 J\mathrm{tr}\boldsymbol{D}^p d\tau \tag{2}$$

here $\mathrm{D} = (\tilde{\lambda}-\tilde{\kappa})/\mathrm{M}/(1+\mathrm{e}_0)$ is the dilatancy coefficient, $\boldsymbol{D}^p$ is the plastic stretching, and $J = (1+\mathrm{e})/(1+\mathrm{e}_0)$, where e is the void ratio at time $t = t$. η^* is given by the following equation using rotational hardening variable $\boldsymbol{\beta}$ and effective stress tensor $\boldsymbol{T}'$ (the tensile components are defined as positive).

$$\eta^* = \sqrt{3/2\,\hat{\boldsymbol{\eta}}\cdot\hat{\boldsymbol{\eta}}},\ \hat{\boldsymbol{\eta}} = \boldsymbol{\eta}-\boldsymbol{\beta},\ \boldsymbol{\eta} = \boldsymbol{S}/p',\ \boldsymbol{S} = \boldsymbol{T}'+p'\boldsymbol{I} \tag{3}$$

The evolution law for the plastic deformation of R^* and R is

$$\dot{R}^* = JU^*\left\|\boldsymbol{D}_s{}^p\right\|,\ U^* = \frac{a}{\mathrm{D}}R^{*b}(1-R^*)^c,\ \dot{R}^* > 0 \tag{4}$$

$$\dot{R} = JU\left\|\boldsymbol{D}^p\right\|,\quad U = -\frac{m}{\mathrm{D}}\ln R,\ \dot{R} > 0 \tag{5}$$

These equations show how R and R^* increase with the development of plastic deformation (loading), and eventually approach 1. $\boldsymbol{D}_s{}^p$ denotes the shear component of the plastic stretching tensor, and $\|\ \|$ indicates the norms. In Eq. (4), $\boldsymbol{D}^p$ is applied to the case of clay. From Eqs. (1) and (2), Eq. (2) shows how, as loading continues and R and R^* approach 1, the soil is remolded until it finally reverts to the normal consolidation state. Further, in both equations, we see that the loss of overconsolidation ($R\to 1$) brings a volumetric expansion of the soil, whereas the decay of structure ($R^*\to 1$) brings a volumetric compression. $1/R$ expresses the overconsolidation ratio (OCR), and $1/R^*$ (>1) the index of structure (the greater the index, the more developed the structure). An explanation of the evolution law for $\boldsymbol{\beta}$ and the axis of anisotropic rotation (Fig. 2) are omitted in the present study.

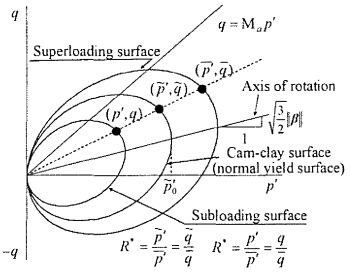

Figure 2. Three loading surfaces.

By applying the associated flow rule and other rules of elasticity to Eq. (1), we are able to obtain the plastic multiplier λ (Eq. (6)) and the constitutive equation (Eq. (10)), as shown below. $\boldsymbol{E}$ is the elastic tensor, $\overset{\circ}{\boldsymbol{T}}{}'$ is the Dienes rate of $\boldsymbol{T}'$, and Λ expresses the plastic multiplier λ under stretching $\boldsymbol{D}$.

$$\lambda = \frac{\dfrac{\partial f}{\partial \boldsymbol{T}'}\cdot\overset{\circ}{\boldsymbol{T}}{}'}{J\dfrac{\mathrm{MD}}{p'(\mathrm{M}^2+\eta^{*2})}(\mathrm{M_s}^2-\eta^2)} \tag{6}$$

$$\mathrm{M_s}^2 = \mathrm{M}_a{}^2 + br\frac{4\mathrm{M}\eta^{*2}}{\mathrm{M}^2+\eta^{*2}}\left(m_b\eta^* - \sqrt{\frac{3}{2}}\hat{\boldsymbol{\eta}}\cdot\boldsymbol{\beta}\right) - \mathrm{MD}\left(2\frac{U^*}{R^*}\eta^* - \frac{U}{R}\sqrt{6\eta^{*2}+\frac{1}{3}(\mathrm{M}_a{}^2-\eta^2)^2}\right) \tag{7}$$

$$\mathrm{M}_a{}^2 = \mathrm{M}^2 + \zeta^2 \tag{8}$$

$$\zeta = \sqrt{\frac{3}{2}\boldsymbol{\beta}\cdot\boldsymbol{\beta}} = \sqrt{\frac{3}{2}}\|\boldsymbol{\beta}\| \tag{9}$$

$$\overset{\circ}{\boldsymbol{T}}{}' = \boldsymbol{E}\boldsymbol{D} - \Lambda\boldsymbol{E}\frac{\partial f}{\partial \boldsymbol{T}'} \tag{10}$$

2.2 *Differences between clay and sand*

The term M_s in Eq. (7) is important because the straight line $q = \mathrm{M}_s p'$ in the stress space $p'\sim q$ gives the boundary between hardening (the area below the line) and softening (the area above). An important point to grasp here is that $\mathrm{M}_s = \mathrm{M}_s(R, R^*, \boldsymbol{\beta}, \eta)$ is a variable, and that M_s is made smaller by a loss of overconsolidation ($R\to 1$) and larger by a decay of structure ($R^*\to 1$).

When sand and clay are subjected to the same plastic deformation, sand will generally show a rapid decay of structure, but its loss of overconsolidation will be extremely slow. Consequently, even if the straight line $q = \mathrm{M}_s p'$ begins in an extremely low initial position, it will first perform an abrupt leap upward due to the breakdown of the structure (increase in M_s) causing the area of hardening to extend above the critical state line (CSL) $q = \mathrm{M}p'$ (hardening above the CSL), before the loss of overconsolidation causes it to drop down again, very slowly indeed, so as to fall together once more with the CSL. This sequence is shown in Fig. 3. Thus, for example, the undrained shearing behavior of medium dense sand can be represented as in Fig. 4. This is an abbreviated account, which omits the issue of anisotropy, but the idea it gives of a rapid decay of structure followed by a gradual loss of overconsolidation helps toward an

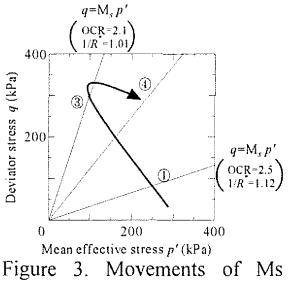

Figure 3. Movements of Ms (sand).

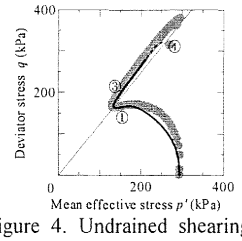

Figure 4. Undrained shearing response.

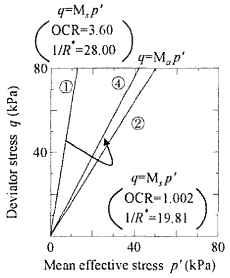

Figure 5. Movements of Ms (clay).

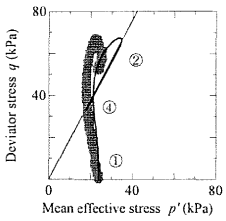

Figure 6. Undrained shearing response.

understanding of the typical behavior of sand in continuing to harden while displaying plastic expansion above the CSL.

Unlike sand, clay requires a great deal of plastic deformation to produce any structural decay, but its loss of overconsolidation will often be relatively rapid. Even where a structured clay exists in a heavily overconsolidated state, so that the line q=M$_s$ p' is in an extremely high starting position, the loss of overconsolidation will first cause it to fall below the critical state line q=Mp' (decrease in M$_s$) so that softening becomes a possibility even beneath the CSL. This is shown in Fig. 5. Thus, when a clay with a high degree of structure and in a state of heavily overconsolidation is subjected to an undrained shearing load, even if the plastic expansion is initially accompanied by hardening above the CSL, there will sooner or later be a switch to softening, and then ultimately to softening together with plastic compression. This can be seen in Fig. 6. This stress path is known as "rewinding," and was first noticed by Tatsuoka et al. (1995).

As the sand and clay samples for Figs. 4 and 6 have the same initial conditions and elasto-plastic parameters as the materials used in chapters 3 and 4 below, explanations of these details can be dispensed with here. But it is to be stressed that the rates of structural decay and overconsolidation loss in the model are controlled by the values of the parameters in the evolution laws for R and R*. There is therefore no need of separate models to represent sand and clay.

3 THE COMPACTION OF SAND AND THE SHEARING CHARACTERISTICS OF SAND IN VARIOUS DENSITIES

Calculations were performed for a drained triaxial compression and extension test with constant lateral pressure on a very loose sand subjected to a repeated shear stress of q=60kPa, using the material constants shown in Table 1. Fig. 7(a) shows the effective stress path, and Fig. 7(b) the volumetric compression due to the repeated shearing. The compaction/densification of the sand is described with this single set of elasto-plastic parameters and

Table 1. Material constants and initial conditions for loose sand.

Elasto-plastic parameters		Evolution parameters		Initial conditions	
M	1.00	m	0.08	p'_0	294 kPa
N	0.97	a (b,c)	2.3(1.0,1.0)	v_0	1.92
$\tilde{\lambda}$	0.05	b_r	200.0	$1/R_0$	1.0
$\tilde{\kappa}$	0.012	m_b	0.7	$1/R^*_0$	100.0

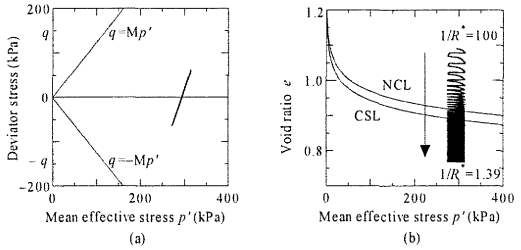

Figure 7. Response of loose sand to a repeated drained shear test.

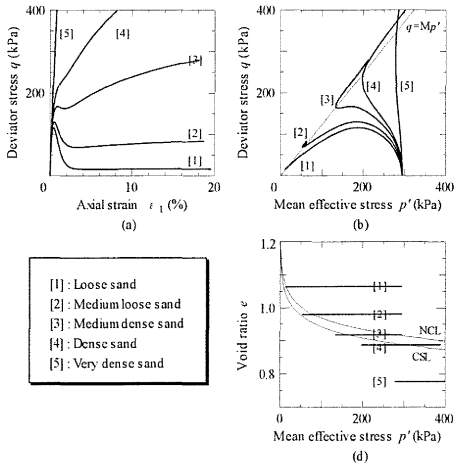

Figure 8. Response to an undrained triaxial compression test following a repeated drained shearing test.

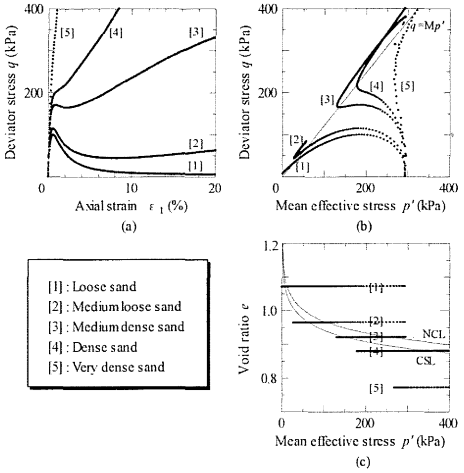

Figure 9. Results of an undrained triaxial compression test after compaction (actual experiment).

evolution laws, using the initial conditions of the loose sand as the only data. The decrease in the structure index $1/R$* and the accumulation in the OCR were computed automatically during the repeated shearing process, and it was found that the loose sand corresponded to a highly structured, normally consolidated soil, while the dense sand showed a less structured and an heavily overconsolidated soil.

Figure 8 gives calculated results for an undrained compression test performed under constant lateral pressure on five densities of sand ([1] – [5]) from very loose to very dense. For comparison, Fig. 9 gives experimental results. The values in the two figures agree closely, qualitatively and quantitatively.

4 LARGE-SCALE COMPRESSION OF CLAY UNDER A REPEATED DRAINED SHEARING LOAD

Figure 10 shows the results of tests performed on two samples of (presumably uniform) clay taken from the Kanda section of Joban Expressway (Asaoka et al., 2005). The samples are subjected to reconsolidation at two different levels of consolidation pressure, followed by undrained shearing. The results are then aligned with calculated values derived from the model in section 2. The elasto-plastic parameters for the calculation are obtained from remolded clay, the evolution parameters, together with the initial conditions for sample A, are determined from the undrained shearing test for that sample (Table 2), while the behavior of sample B is predictions. The matches with the measured results are not as good as for the sand tests, but the

Table 2. Material constants and initial conditions for clay.

Elasto-plastic parameters		Evolution parameters		Initial conditions	
M	1.65	m	1.2	p'_0	24.0kPa
N	2.80	a (b,c)	0.01(1.0,7.5)	v_0	3.65
$\tilde{\lambda}$	0.28	b_r	0.01	$1/R_0$	3.95
$\tilde{\kappa}$	0.047	m_b	1.6	$1/R^*_0$	29.24

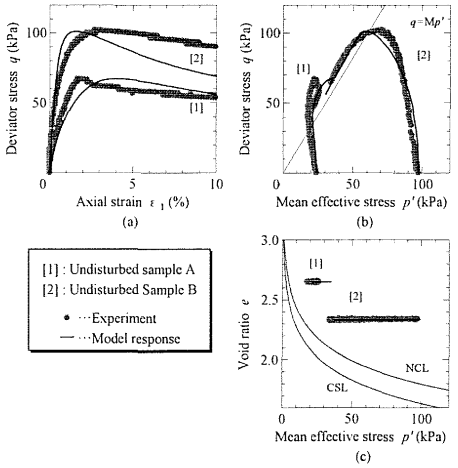

Figure 10. Experimental and calculated results for undrained triaxial compression tests on clay.

changes in the strength and shear characteristics are qualitatively well described.

Figure 11 shows a pattern of continuous long-term, large-scale settlement in an alluvial soft clay soil as a result of embankment work on the Kanda section of the Joban Expressway. As can be seen from the figure, settlement is still continuing at present, more than 20 years after the completion of the embankment. The 'calculation' is used by an elasto-plastic deformation analysis under the plane strain condition, based on the parameters for clay in the preceding section. As the (A)→(B)→(C) part of the figure shows, the settlement can be expected to go on occurring into the future. Let us now take a simple look at what the model and calculation can tell us if we focus on point a in the Fig. 11 section diagram, located at mid-depth in the clay layer immediately beneath the embankment. Fig. 12 (a) shows the vertical effective stress path of point a against specific volume, and Fig. 12 (b) the mean effective stress path, again at point a. The calculation in Fig. 12 (a), as can be confirmed by comparing the 'applied loading' along the path (A)→(B), reveals that in the 20 years or so until (C), while there is hardly any dissipation of pore water pressure, the structure of the clay is disturbed by complicated repetitions of drained shearing leading to occurrences of large-scale compression. On reaching point (C) the structure in this soil still exists, and the settlement can be expected to go on occurring by another kind of loading.

The complicated repeated shearing between points (A) and (C) reflects a progressive collapse of structure in the layer of clay. As softening occurs in one soil element, since the load remains constant, there is a rise in pore water pressure resulting in an unloading onto other adjoining soil elements. Later, as this soil element reverts back to hardening, the adjoining elements will change over to softening, producing an alternation in each of them between hardening and softening, loading and unloading, which gives rise to the kind of complex stress path found in Fig. 12 (b).

The compression behavior in clay as shown in Fig. 12 (a), which is similar to the result for sand in Fig. 7, means that even for clay '**compaction**' occurs due to decay of the structure. This Joban Expressway site is by no means unique as an example of long-term, large-scale continuous settlement occurring without appreciable dissipation of pore water pressure. Plenty of similar cases have been encountered in practical engineering experience.

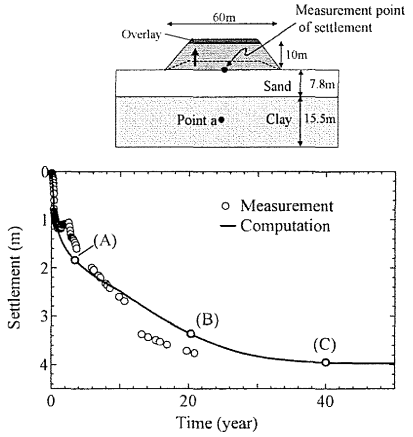

Figure 11. Actual measurements and calculated projections of settlement.

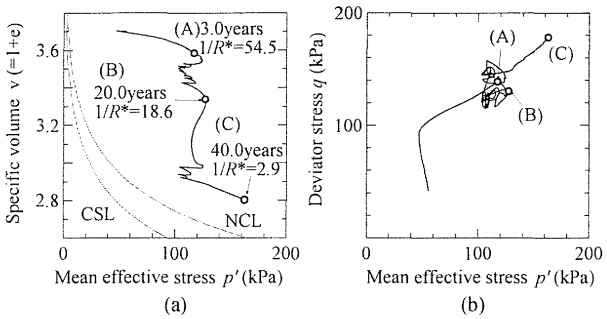

Figure 12. Compression behavior and effective stress path at point a.

5 CONCLUSIONS

The co-occurrence of large-scale soil compression with decay in the soil skeleton structure is a striking phenomenon both in sand and in clay, in laboratory tests and in-site observations. Repeated drained shearing, and decay of the skeleton structure, lead to compaction in sand, and to large-scale compression in clay. The use of an elasto-plastic constitutive equation which is capable of accounting at once for the decay of skeleton structure and the loss of overconsolidation makes it possible to give a mechanical description of these phenomena, and this description can be of great service in helping geo-engineers to enhance their intuitive understanding.

REFERENCES

Asaoka, A. et al. 2000. Superloading yield surface concept for highly structured soil behavior. *Soils and Foundations*, 40, 2, 99-110.

Asaoka, A. et al. 2002. An elasto-plastic description of two distinct volume change mechanics of soils. *Soils and Foundations*, 42, 5, 47-57.

Asaoka, A. et al. 2005. Progressive consolidation of highly structured clay under embankment loading. *Proc.16th Int. Conf. on Soil Mechanics and Geotechnical Engineering*, Osaka, to appear.

Sekiguchi, H. and Ohta, H. 1977. Induced anisotropy and time dependency in clays. *Constitutive Equations of Soils (Proc, 9th Int. Conf. Soil Mech. Found. Eng., Spec. Session9)*, Tokyo, 229-238.

Hashiguchi, K. and Chen, Z. -P. 1998. Elastoplastic constitutive equations of soils with the subloading surface and the rotational hardening. *Int. J. Numer. Anal. Meth. Geomech.*, 22, 197-227.

Hashiguchi, K. 1989. Subloading surface model in unconventional plasticity. *Int. J. of Solids and Structures*, 25, 917-945.

Tatsuoka, F. and Kohata, Y. 1995. Stiffness of hard soils and soft rocks in wngineering applications. *Proc. of 1st int. conf. on Pre-failure deformation characteristics of geomaterials*, Sapporo, 2, 947-1063.